Green synthesize of fly ash-based zeolite X: A potential microwave absorbent

Bin Shi
Yan'an University
Junjie Zhao
Fujian Institute of Geological Survey
Qing Chang (changqingyau@126.com)
Yan'an University https://orcid.org/0000-0002-9153-2509

Research Article

Keywords: Zeolite X, Fly ash, Green synthesis, Dielectric absorber.

Posted Date: February 24th, 2021

DOI: https://doi.org/10.21203/rs.3.rs-233778/v1

Abstract

Zeolite X is a potential electromagnetic wave (EMW) absorption material owning to its advantages of good dielectric properties, light weight and large specific surface area. Herein, high-purity zeolite X was prepared from fly ash using a green synthesis approach, in which only trace water was used and achieved zero discharge of waste water. Physiochemical properties of fabricated zeolite X were comprehensively evaluated through XRD, PSD, SEM, TG-DSC and BET test. XRD pattern shows the successful preparation of zeolite X with good crystallinity and high purity, and the average particle size is ~2.45 μm, which conforms to Gaussian distributions. The fabricated zeolite X exhibits typical octahedral structure and good thermal stability. It is noteworthy that the specific surface area is up to 473.56 m 2 /g, representing porous structure, which is beneficial to EMW attenuation. What's more, the abundant crystal water and adsorbed water existing in the sample is conductive to dipole polarization, which further consume EMW energy. This study provides an eco-friendly approach to change waste into valuables, and moreover the synthesized zeolite X is a potential EMW absorbing material.

1. Introduction

With the wide use of electronic devices, electromagnetic wave (EMW) pollution is becoming more and more serious, and hence EMW absorbing materials have attracted wide attention [1-2]. So far, various materials have already been prepared for EMW adsorption [3-10]. As a kind of low-cost material, natural and synthetic zeolites have great application potential in EMW adsorption field owning to the advantages of unique dielectric properties, low density, high specific surface, and strong mechanical and chemical stability. Recently, Shang et al. reported a sepiolite-based EMW adsorption composites with superior EMW absorption performance, in which the minimum reflection loss of -50.23 dB and effective absorption bandwidth of 5.01 GHz [11]. Using low-cost light-weight and natural sepiolite as starting material, the synthesis procedure is facile, economic and commercially practical. What's more, the large surface area of sepiolite is convenient for multiple reflections and scattering, which can increase the propagation path of incident EMW and promote EMW dissipation. As another kind of porous mineral material, the research of zeolite/zeolite-based materials as islanding or regional dielectric loss absorbers is of great significance in the research field of new EMW absorbing materials, while the relevant reports are still rare.

Zeolite X is one of the most widely used zeolites due to its large specific surface area and high adsorption capacity [12-14]. As a kind of porous inorganic material, zeolite has the characteristics of crystal and open framework structure with many pores in it. These pores are connected with each other through channels, and the pore size distribution is highly uniform. The weak interaction between porous AlO_4/SiO_4 structure and non-framework cations endows zeolite with unique dielectric properties. The characteristics above are beneficial to EMW loss. Fly ash, a solid waste with huge discharge, has been widely used for the synthesis of zeolite X owing to its high silicon and aluminum content [15-17]. Numerous studies have been established to synthesize zeolite X, such as one-step method [18-19], two-step method [20-21], microwave-assisted two-step method [22-23] and ultrasonic-assisted method [24]. Normally, a large amount of solvent involves water or organic solution is required in these processes,

which inevitably results in wastewater pollution [25]. In light of this, a pioneering process of solvent-free (trace water system) approach is proposed to solve this problem [26]. As a green approach, solvent-free method possesses significant advantages as high yield, sufficient utilization of autoclaves, and reduction of pollutants and so on [27].

In this study, low-cost zeolite X was synthesized from fly ash using a solvent-free method. The prepared zeolite X possesses outstanding physical and chemical properties, and notably, the specific surface area is up to 473.56 m^2/g, which represents porous structure and is beneficial to EMW attenuation. The work supplied a green and low-cost method to prepare zeolite X, which was expected to be an EMW absorbing material.

2. Experimental

2.1. Materials

In this work, fly ash was obtained from Inner Mongolia, China. Analytical purity sodium aluminate, sodium hydroxide and sodium silicate were purchased from Aladdin reagent Co., Ltd.

2.2. Synthesis of zeolite X

As we can see from XRF results (Table S1), Si/Al in fly ash is 1.70 which exhibits ideal raw materials for the synthesis of zeolite X, and no additional Si or Al source was necessary. The synthesis process was conducted in the following steps: Firstly, fly ash was homogeneously mixed with sodium hydroxide and the mixture was calcined in muffle furnace at 750℃ for 2h. After cooling, trace amounts of water and prepared seeds (5% wt) were added into the fused mixture to make a smooth paste. The final molar ratio of Na:Al:Si:H_2O is 1:1:1.6:3.5 (in accordance with typical zeolite X (JCPDS card No. 12-0228): $Na_2Al_2Si_{3.3}O_{10.6}{\cdot}7H_2O$). Then transferred the paste into autoclave, and heating in an oven at 120℃ for 12-72h. After that, filtered and washed with distilled water for three times. Finally, the solid was dried at 105℃ for 24 h, and Zeolite X powder was obtained. The scheme of the synthesis process was shown in **Fig. 1**.

2.3. Characterization

Elements of raw ore, synthesized zeolite X and residue were tested by X-ray fluorescence spectrometer (XRF, $AXIOS^{Max}$, PANalytical). The phase structure of the samples were analyzed by X-ray Diffractionmeter (XRD, D8-FOCUS, Bruker). Morphological characteristics were performed by a Scanning Electron Microscope (SEM, SU8010, HITACHI). The particle size distribution (PSD) of samples were determined using laser particle size analyzer instrument (Mastersizer 2000, MALVERN). The Brunauer-Emmett-Teller (BET) surface area, pore volume and pore size distribution were performed by N_2 adsorption at 77 K with an ASAP2020 (TSI) Automatic Volumetric Sorption Analyzer. Thermogravimetry/Differential Scanning Calorimetry (TG-DSC) analyses were characterized by Netzsch STA 409 thermal analysis system.

3. Results And Discussion

3.1. XRD patterns and XRF analysis of synthesized zeolites

To rapidly obtain pure zeolite X, synthesis time was controlled between 12h and 72h. When the reaction time is 12h, the product is completely amorphous. Then raising the reaction time to 24h, zeolite X (JCPDS card No. 12-0228) with low crystallinity and zeolite P (JCPDS card No. 39-0219) are obtained, and the content of zeolite X is higher than zeolite P. Thus, continuing to increase the reaction time to 48h, zeolite X with high crystallinity is prepared. Although there is still tiny amount of zeolite P, the purity and crystallinity are excellent enough. Further improving the reaction time to 72h, intensity of zeolite X weakens remarkably, however, intensity of zeolite P strengthens by contrast. In addition, peaks of sodalite (JCPDS card No. 73-1733) appear as well. It is obvious that high temperature is unfavorable to the crystallization of zeolite X. Therefore, zeolite X synthesized at 48h is taken for the further study, which is named SZX.

X-ray fluorescence spectrometer (XRF) was used to conduct the chemical compositions of SZX. As is shown, apart from the structural components of zeolite X (Si, Al and Na), small amount of Ti, Fe, Mg, Ca, K are also concluded. The Si/Al ratio of SZX is 1.28, presents a typical zeolite X. (**Table 1**).

Table 1. Main compositions of SZX, *LOI is loss on ignition.* (mass fraction, %)

Composition	SiO_2	Al_2O_3	Na_2O	TiO_2	TFe	MgO	CaO	K_2O	LOI
Wt.%	39.36	26.15	15.91	0.04	0.06	0.26	0.31	0.26	16.92

3.2. Morphology analysis of synthesized zeolites

The SEM images and EDS result are shown in Fig. 3. When the reaction time is 24h (Fig.3(a)), it can be seen that the particle size of zeolite X is about 2.5μm, and the morphology is irregular. Thus, continuing to increase the reaction time to 48h (Fig.3(b)), the morphology of zeolite X is of regular octahedron and uniform particle size (about 2.5μm). Zeolite X synthesized at 72h presents regular octahedron as well (Fig.3(c)), but the particle size (about 2.6μm) is a little larger than that of 48h. The EDS result of SZX is exhibited in Fig. 2(d), and it shows that the Si/Al ratio is about 1.28, which fits the XRF result perfectly.

3.3. Particle size distribution of synthesized zeolites

According to the data of PSD (Fig. 2(f)), the particle size distribution of SZX follows gaussian distributions, and the average particle size of SZX is about 2.45μm, which was in good agreement with the SEM results. The results above indicate that SZX was smaller and more uniform compared to that obtained by hydrothermal method [28-29].

3.4. Thermal behavior analysis

TG-DSC curves of SZX are shown in Fig. 5. Before 100℃, there is a weak endothermic peek, which shows adsorbing steam of air on SZX [30]. TG curve of the sample shows smooth mass loss and was devoid of any distinct kinks. And a significant endothermal valley appears at 136℃. Meanwhile, there is a dramatic weight loss on the TG curve. When it reaches to 246℃, the free water is removed completely. Obviously, the content of free water is high, which will produce dipole polarization and relaxation under the action of electromagnetic field so as to consume EMW energy. The strong exothermal peak at 246℃ may be caused by the combustion of organic impurities, which is another source of dipole polarization. After 600℃, mass loss is stable at about 20.61%. Although the TG-DSC analysis was conducted under 800℃, however, the tendency of DSC curve hints that there exists at least an exothermal peak after 800℃ which is caused by the phase transformation and the decomposition of zeolite structure [31]. Hence the heat treatment temperature of SZX should be controlled below 600℃.

3.5. Specific surface area analysis

The pore structure of SZX was evaluated by nitrogen adsorption measurements, and the results are shown in Fig.6. According to the IUPAC classification, the isotherm presents classical type IV with H3 hysteresis loop [32,33]. The pore size distribution for SZX was estimated by the BJH method as shown in the insert Fig. 6, which shows a pore radius below 3 nm. And the broad pore size distribution might be caused by the agglomeration of zeolite particles. The textural parameters of SZX are shown in Table 2. BET surface area is measured to be 473.56 m^2/g, and the prepared zeolite is primarily microporous with average pore size of 1.914 nm. Large numbers of micropores and channels allows EMW transmit into the material easily, and extends the propagation channel of EMW. Thus, EMW adsorption is increased. According to the literatures, large specific surface area of porous material represents good EMW absorbing performance.

Table 2. Textural Parameters of SZX

	S_{BET} (m^2/g)	S_{mic} (m^2/g)	V_{Total} (cm^3/g)	V_{mic} (cm^3/g)	Average pore size (nm)
MSZX	473.56	428.32	0.265	0.240	1.914

3.6. Prospect as an EMW absorbent

The zeolite X prepared in this work is of good prospect to be EMW absorbing materials. On one hand, the special porous structure and frame structure enable zeolite X good impedance matching, which make the incident EMW enter the material as much as possible; on the other hand, in addition to dipole polarization loss caused by adsorbed water and impurities, the vesicular cavity and the structure between vesicular in materials will also reflect and scatter EMWs, which dissipate EMW energy greatly. What's more, Zeolite materials have the characteristics of light weight and thermal stability, which provides favorable conditions for it to become a new type of microwave absorbing material. Briefly, the zeolite X prepared in this work is of good prospect to be a EMW absorbing material. So zeolite and zeolite-based materials will be further studied in our following work.

4. Conclusions

High purity zeolite X was synthesized by a green methed from fly ash in 48h. For SZX, the Si/Al ratio is 1.28; the average particle size is about 2.45μm; and the specific surface area is 473.56 m^2/g. Besides, the SZX shows good phase, morphology and thermal stability as well. Besides, through theoretical analysis, zeolite X is a hopeful EMW absorbing material because of its good impedance matching, dipole polarization loss and reflecting and scattering EMWs caused by vesicular cavity. And the EMW adsorption capacity of zeolite X will be further studied in following research.

Declarations

The authors declare that they have no known competing financial interests or personal relationships that could have appeared to influence the work reported in this paper.

Acknowledgement

This study was funded by the Research Program of Yan'an University (Grant No. YDY2019-25).

References

[1] A. Iqbal, F. Shahzad, K. Hantanasirisakul, Science **369**, 446 (2020) https://doi.org/10.1126/science.aba7977.

[2] I. Abdalla, A. Elhassan, J.Y. Yu, Carbon **157,** 703-713 (2020) https://doi.org/10.1016/j.carbon.2019.11.004.

[3] H.J. Wu, L.D. Wang, S.L. Guo, Appl. Phys. A. **108,** 439-446 (2012) https://doi.org/10.1007/s00339-012-6906-6.

[4] H.S. Liang, H. Xing, M. Qin, Compos. Part A-Appl. S. **135,** 105959 (2020) https://doi.org/10.1016/j.compositesa.2020.105959.

[5] D. Lan, M. Qin, J.L. Liu, Chem. Eng. J. **382,** 122797 (2020) https://doi.org/10.1016/j.cej.2020.127313.

[6] H.J. Wu, M. Qin, L.M. Zhang, Compos. Part B-Eng. **182,** 107620 (2020) https://doi.org/10.1016/j.compositesb.2019.107620.

[7] Q. Chang, H. Liang, B. Shi, J. Colloid Interf. Sci. **588,** 336-345(2021) https://doi.org/10.1016/j.jcis.2020.12.099.

[8] M. Qin, L. Zhang, X. Zhao, Adv. Sci. 2004640 (2021) https://doi.org/10.1002/advs.202004640.

[9] H. Liang, J. Liu, Y Zhang, Compos. Part B-Eng. **178,** 107507 (2019) https://doi.org/10.1016/j.compositesb.2019.107507.

[10] G. Chen, L. Zhang, X. Fan, J. Colloid Interf. Sci. **588,** 813-825 (2021) https://doi.org/10.1016/j.jcis.2020.11.117.

[11] Q. Shang, H. Feng, Z. Feng, J. Colloid Interf. Sci. **576,** 444-456 (2020) https://doi.org/10.1016/j.jcis.2020.05.052.

[12] T. Zhu, X. Zhang, Y. Han, Front. Chem. **7,** 341 (2019) https://doi.org/10.3389/fchem.2019.00341.

[13] S. Bai, M. Chu, L. Zhou, Energ. Source. Part A. 1-11 (2019) https://doi.org/10.1080/15567036.2019.1661549.

[14] C. Han, T. Yang, H. Liu, Environ. Sci. Pollut. R. **26**, 10106-10116 (2019) https://doi.org/10.1007/s11356-019-04466-x.

[15] Y. Liu, Q. Luo, G. Wang, Mater. Res. Express **5,** 055507 (2018) https://doi.org/10.1088/2053-1591/aac3ae.

[16] T. Yang, C. Han, H. Liu, Adv. Powder Technol. **30,** 199-206 (2019) https://doi.org/10.1016/j.apt.2018.10.023.

[17] Z. Tauanov, D. Shah, V. Inglezakis, J. Clean. Prod. **182,** 616-623 (2018) https://doi.org/10.1016/j.jclepro.2018.02.047.

[18] A. Grela, M. Hebda, M. Łach, Microporous Mesoporous Mater. **220,** 155-162 (2016) http://dx.doi.org/10.1016/j.micromeso.2015.08.036.

[19] M. Osacký, H. Pálková, P. Hudec, Microporous Mesoporous Mater. **294,** 109852 (2020) https://doi.org/10.1016/j.micromeso.2019.109852.

[20] R.V. De La Villa Mencía, E. Goiti, M. Ocejo, R.G. Giménez, Microporous Mesoporous Mater. **293,** 109817 (2020) https://doi.org/10.1016/j.micromeso.2019.109817.

[21] Z. Qiang, R. Li, Z. Yang, Energ. Fuel. **33,** 6641-6649 (2019) https://doi.org/10.1021/acs.energyfuels.9b01268.

[22] Y. Fang, T. Shi, X. Liang, Microporous Mesoporous Mater. **294**, 109900 (2020) https://doi.org/10.1016/j.micromeso.2019.109900.

[23] T. Le, Q. Wang, B. Pan, Microporous Mesoporous Mater. **284,** 476-485 (2019) https://doi.org/10.1016/j.micromeso.2019.04.029.

[24] S. Sivalingam, S. Sujit, Environ. Sci. Pollut. R. **26,** 34693-34701 (2019) https://doi.org/10.1007/s11356-018-3664-9.

[25] C.S. Cundy, P.A. Cox, Chem. Rev. **103,** 663-702 (2003) https://doi.org/10.1021/cr020060i.

[26] Q. Wu, X. Meng, X. Gao, Acc. Chem. Res. **51,** 1396-1403 (2018) https://doi.org/10.1021/acs.accounts.8b00057.

[27] W. Luo, X. Yang, Z. Wang, Microporous Mesoporous Mater. **243,** 112-118 (2017) https://doi.org/10.1016/j.micromeso.2017.01.040.

[28] J.L.X. Hong, T. Maneerung, S.N. Koh, S. Kawi, Ind. Eng. Chem. Res. **56,** 11565-11574 (2017) https://doi.org/10.1021/acs.iecr.7b02885.

[29] H. Tanaka, A. Fujii, Adv. Powder Technol. **20,** 473-479 (2009) https://doi.org/10.1016/j.apt.2009.05.004.

[30] S.H. Wu, C.C. Hsieh, C.C. Chiang, J. Therm. Anal. Calorim. **109,** 945-950 (2012) https://doi.org/10.1007/s10973-011-1825-x.

[31] M. Xiao, X. Hu, Y. Gong, RSC Adv. **5,** 100743-100749 (2015) https://doi.org/10.1039/C5RA17856H.

[32] N. Koshy, D.N. Singh, J. Environ. Chem. Eng. **4,** 1460-1472 (2016) https://doi.org/10.1016/j.jece.2016.02.002.

[33] H. Wang, Q. Chang, F. Zhou, Sci. Adv. Mater. **11,** 60-67 (2019) https://doi.org/10.1166/sam.2019.3387.

Figures

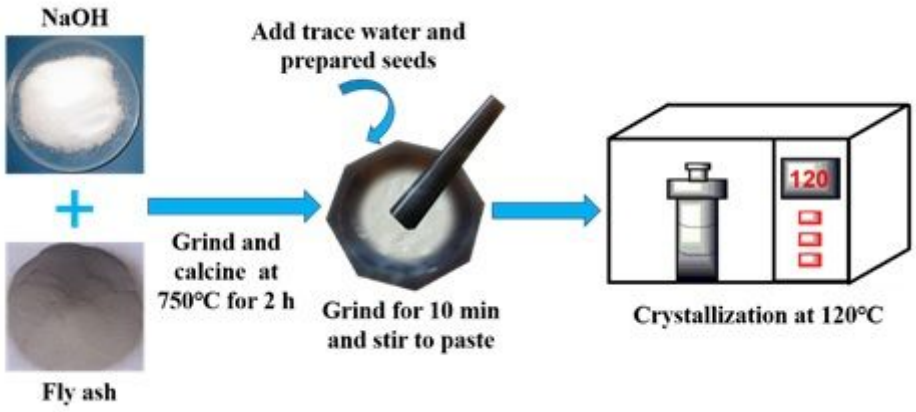

Figure 1

The scheme of synthesize zeolite X.

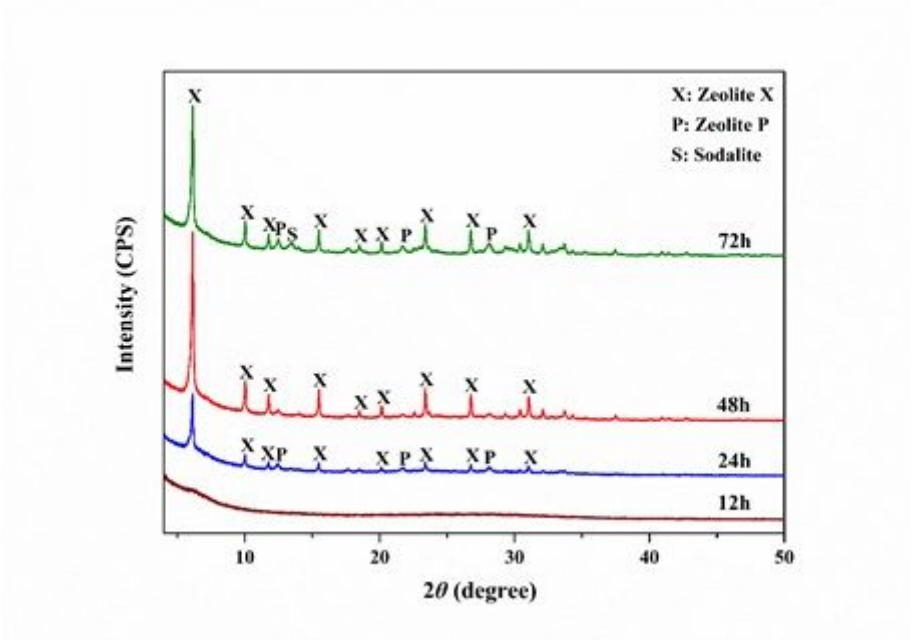

Figure 2

XRD patterns of products synthesized at different crystallization time.

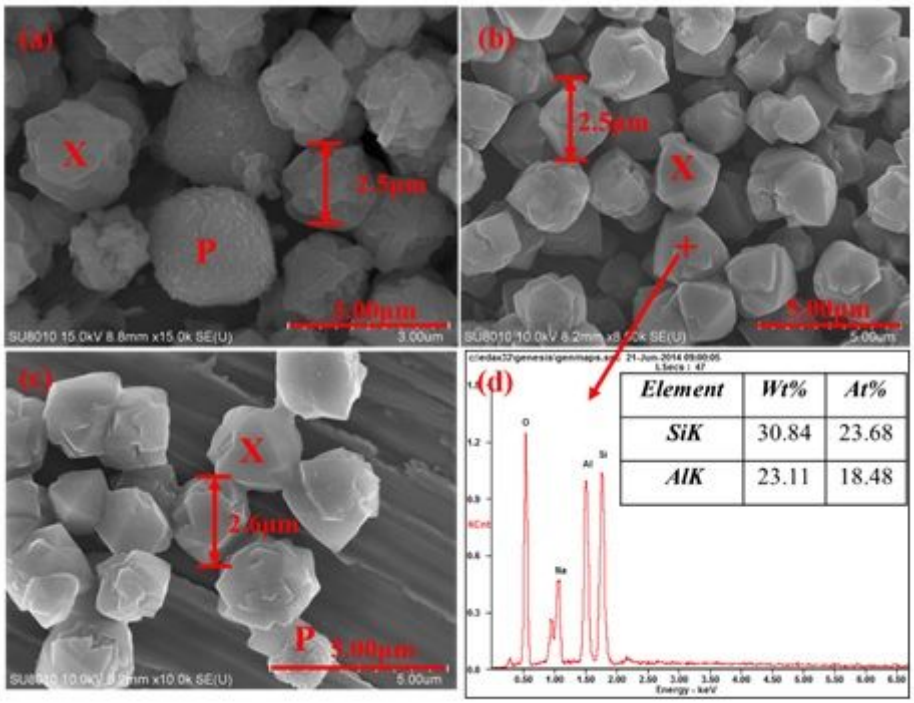

Figure 3

SEM images of zeolites synthesized at (a) 24h, (b) 48h and (c) 72h respectively; (d): EDS result of zeolite (b);

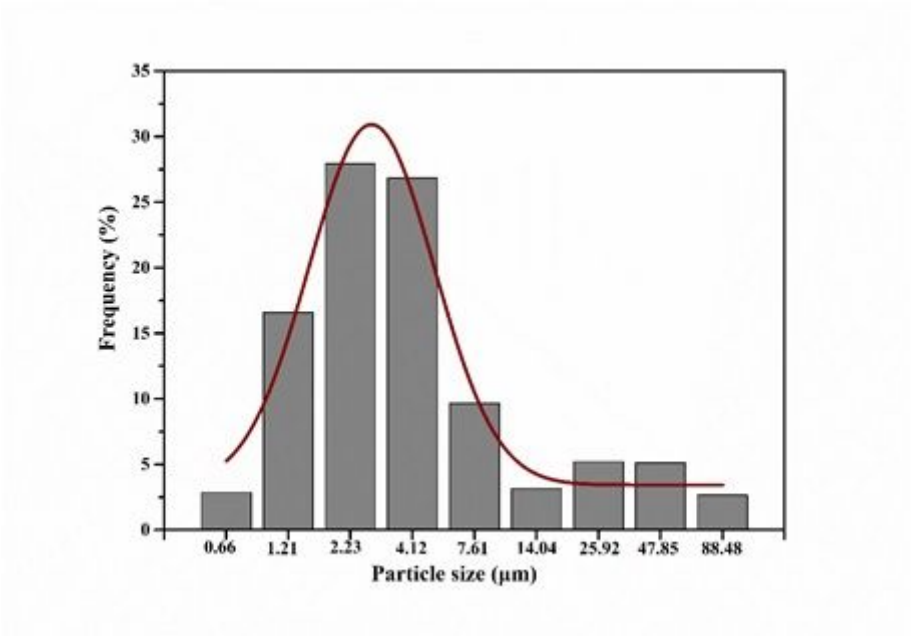

Figure 4

Particle size distribution of zeolite synthesized at 48h.

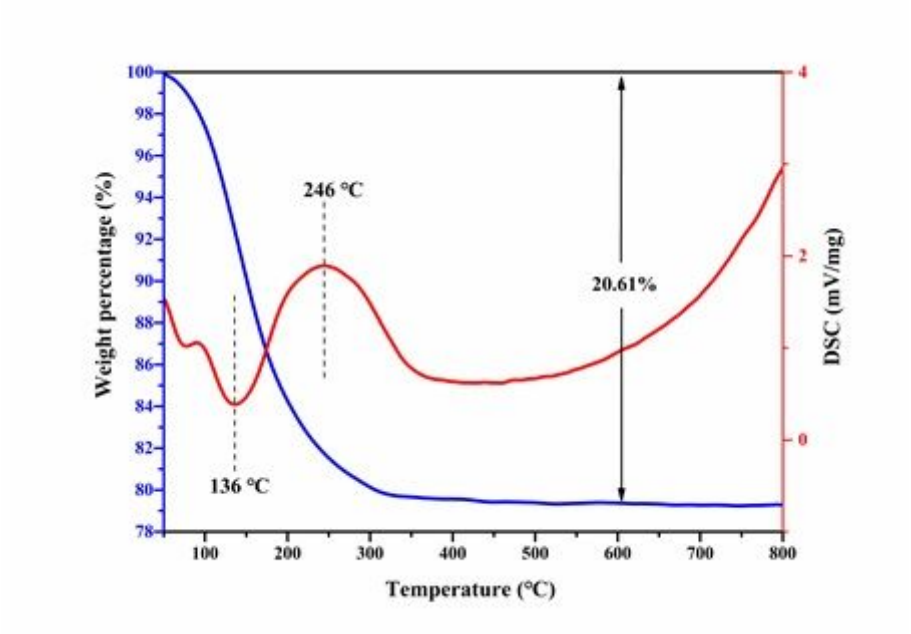

Figure 5

TG-DSC curves of SZX.

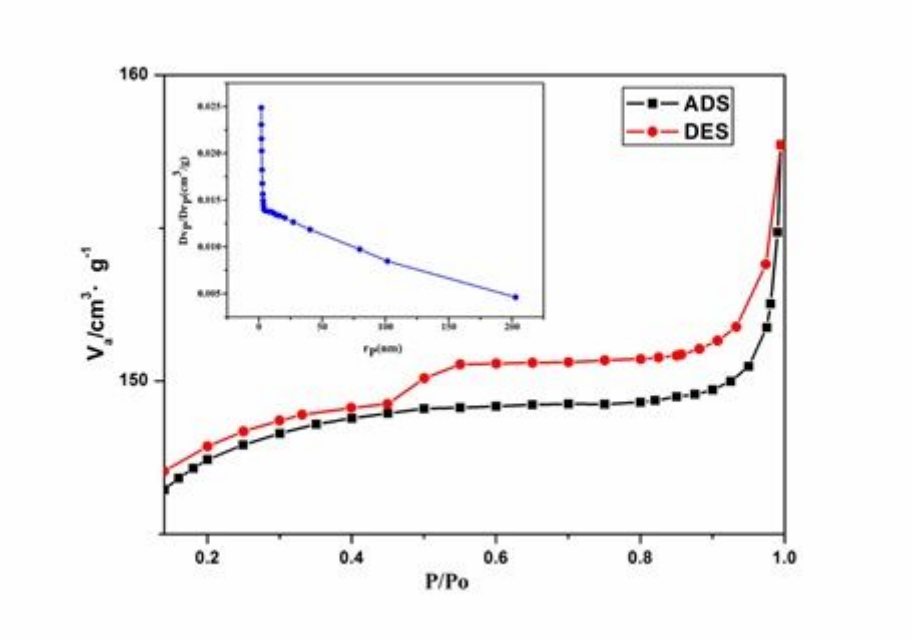

Figure 6

Nitrogen adsorption–desorption isotherms of SZX; Insert is BJH pore size distribution curve.

Supplementary Files

This is a list of supplementary files associated with this preprint. Click to download.

- Supplementarymaterial.pdf